

# EXPLORING THE THERAPEUTIC BENEFITS OF PARTHENIUM HYSTEROPHORUS: ANTIOXIDANT AND ANTICANCER PERSPECTIVES

Gauri Mukesh Nagarkar<sup>[a]</sup>, Pallavi Bajirao Salunkhe<sup>[a]</sup>, Avinash Ashok Survase<sup>[a]</sup>, Geetanjali Vikas Utekar<sup>[a]</sup> \*

<sup>a</sup>Department of Microbiology, Yashavantrao Chavan Institute of Science, Constituent College, Karmaveer Bhaurao Patil University, Satara, 415 001, INDIA

Corresponding Author: G. V. Utekar

Email ID: [ugeeta65@gmail.com](mailto:ugeeta65@gmail.com)

DOI: <https://doi.org/10.63001/tbs.2025.v20.i01.pp583-592>

## KEYWORDS

Parthenium hysterophorus, ZnO Nanoparticles, Anti-oxidant activity, Anti-cancer activity, Phytochemical Study

Received on:

04-01-2025

Accepted on:

04-02-2025

Published on:

11-03-2025

## ABSTRACT

*Parthenium hysterophorus* is a highly invasive annual herb with significant medicinal properties. Traditionally, it has been used to treat various infectious and degenerative diseases. All parts of the plant act as a bitter tonic, febrifuge, emmenagogue, and antidyenteric. It has strong antibacterial, antifungal, antiviral, anti-parasitic, and anthelmintic effects due to its rich bioactive compounds, including flavonoids, polyphenols, alkaloids, terpenes, and pseudoguaianolides. Flavonoids, in particular, provide antioxidative, hepatoprotective, cardioprotective, anti-inflammatory, antiviral, and anticancer benefits. Despite its medicinal value, *Parthenium hysterophorus* is one of the world's most invasive weeds, rapidly colonizing agricultural lands, forests, and disturbed habitats. It produces thousands of seeds each season, spreading aggressively in abandoned areas, roadsides, and irrigation canals, disrupting ecosystems. Recent research highlights its potential in cancer treatment. Zinc oxide nanoparticles (ZnO NPs) derived from the plant show strong antimicrobial and anticancer effects. These nanoparticles selectively kill cancer cells by inducing oxidative stress, mitochondrial damage, and apoptosis while sparing healthy cells. Enhanced ZnO-Ag nanoparticles are even more effective at lower doses, offering promise for cancer therapies, especially where conventional treatments fail. The plant's flower extract, rich in flavonoids and pseudoguaianolides, may help inhibit tumor Growth and trigger cancer cell death. Exploring its medicinal properties could lead to new plant-based cancer treatments. Additionally, developing sustainable, affordable methods to produce safe nanoparticles for medical use may provide a solution for utilizing this invasive species in a beneficial way.

## INTRODUCTION

*Parthenium hysterophorus* was regarded as one of the world's top ten worst terrestrial weeds due to its high reproductive potential. They can grow in a matter of weeks and cover vast agricultural, woodland, and native vegetation areas. This noxious weed is commonly found on abandoned lands, developing residential colonies near towns, railway tracks, roads, drainage and irrigation canals, and so on (Saha et al., 2022). *Parthenium hysterophorus* is a prolific weed in the Asteraceae family that produces thousands of little white capitula, each of which yields five seeds when mature. It is an aggressive annual herbaceous weed that has yet to be discovered to have any commercial value. (Patel, 2011). *Parthenium* presumably entered India around 1910 (via contaminated cereal grain) but went undetected until 1956 (Bagachi et al. 2016). Many infectious and degenerative disorders have been treated using its decoction in traditional medicine. (Kumar et al., 2013b). There are reports of using all portions of the plant as an emmenagogue, febrifuge, bitter tonic, and antidyenteric (Oudhia et al. 2001). An annual and regional herb, *Parthenium hysterophorus* has antibacterial, antifungal, antiviral, anti-parasitic, and anthelmintic qualities.

(Sharif et al. 2021). *Parthenium hysterophorus* includes flavonoids. Flavonoids are a wide class of polyphenolic chemicals that have been demonstrated to have antioxidant, hepatoprotective, cardioprotective, anti-inflammatory, antiviral, and anticancer properties. They are produced by both plants and genetically modified microorganisms (Kumar et al., 2014). *P. hysterophorus* is vital and advantageous due to its therapeutic qualities, which include oils, polyphenols, flavones, flavonoids, alkaloids, terpenes, pseudoguaianolides, and histamines (Jaiswal et al., 2022).

Allelopathic effects are demonstrated by *Parthenium hysterophorus*, which produces phytochemicals such as parthenin and coronopilin that are auto-toxic to its own seed development and growth (Picman et al., 1981). Parthenin, a key chemical in *P. hysterophorus*, is phytotoxic to a variety of plants, including weeds and crops such as *Amaranthus viridis*, *Ageratum conyzoides*, *Avena fatua*, *Chenopodium murale*, *Cassia tora*, and *Phaseolus aureus* (Batish, Singh, Kohli, et al., 2002b ; Batish et al., 2002). It also has various positive qualities, including as antibacterial, antioxidant, cytotoxic, and larvicidal activities against *Aedes aegypti*, as well as applications in muscular relaxation, pest management, bioethanol production,

and the synthesis of silver (Parshar, Vyom et al.2009) and in production of zinc nanoparticles (Rajiv, P et al. 2013). Because of their low risk and few adverse effects, nanoscale materials have a lot of potential for treating cancer. For example, metal-oxide nanoparticles (NPs) are being produced for both detection and treatment. Because of their distinct physicochemical characteristics, biocompatibility, and biodegradability, zinc oxide nanoparticles (ZnO NPs) stand out among them and show great promise in the diagnosis and treatment of a variety of malignancies (Meenakshi et al., 2024). In the fields of biology, medicine, drug delivery, environmental cleanup, and catalysis, zinc oxide nanoparticles have demonstrated exceptional promise. These nanoparticles have been successfully created by researchers using botanical sources (Saini et al., 2024). *Parthenium hysterophorus* is a plant rich in phytochemicals such as alkaloids, phenols, flavonoids, tannins, and saponins, all of which have a variety of biological activities. The plant's high total phenolic and flavonoid content contributes to its antioxidant action by blocking free radicals and increasing enzyme activities (Iqbal, Javed et al.2022 ; Jiménez et al., 2022 ; Kumari & Deepalakshmi, 2017). Furthermore, their anticancer potential has been established by cytotoxic effects on cancer cell lines, with studies demonstrating their effectiveness in triggering cancer cell death by targeting cellular processes (Tanwar et al., 2024). Zinc oxide nanoparticles (ZnO NPs) have shown promising anticancer effects against various cancer cell lines, such as MDA-MB-231 (breast cancer) and K562 (blood cancer), by inducing apoptosis and cell cycle arrest through reactive oxygen species (ROS) generation and mitochondrial disruption. While selectively inhibiting K562 cell growth, ZnO NPs exhibit low toxicity toward normal cells like lymphocytes and renal cells (Anjum et al., 2021 ; Alsagaby et al., 2020). This study explores the potential of Zinc Oxide nanoparticles (ZnO NPs) in various applications, including their antioxidant and anti-cancer properties. Specifically, it examines ZnO NPs synthesized from *Parthenium hysterophorus* using the MTT assay to assess their antitumor effects. The study evaluates their impact on breast cancer (MDAMB231) and blood cancer (K562) cell lines while also testing their effects on normal kidney cell viability.

#### **MATERIAL AND METHOD:**

##### **Sample collection :**

The floral extract of *Parthenium hysterophorus* was obtained from plants collected in Nagthane, Satara District, Maharashtra, India.

##### **Extraction :**

The decoction method was used, where 10 g of washed flowers were soaked in 100 ml of double distilled water at 60°C for 15 minutes. The mixture was then filtered using Whatman filter paper and stored at 4°C for future use.

##### **Synthesis of Nanoparticles :**

The floral extract was mixed with a 1 mM zinc sulfate solution in a 9:1 ratio and incubated for 24 hours, forming zinc oxide nanoparticles (ZnO NPs), indicated by a color change.

##### **Characterization of Nanoparticles :**

ZnO NPs were analyzed using various techniques like UV-Visible Spectroscopy to determine optical properties. Fourier Transform Infrared Spectroscopy (FTIR) to identify functional groups. X-ray Diffraction (XRD) to analyze crystalline structure using the Debye-

Scherrer equation. Scanning Electron Microscopy (SEM) to observe surface morphology, with samples coated in a 4 nm gold layer to prevent charging effects.

#### **Evaluating Biological activities of ZnO Nanoparticles of *Parthenium hysterophorus* :**

##### **Phytochemical analysis :**

Studies have shown that *P. hysterophorus* contains high levels of flavonoids and phenolic compounds (Iqbal, Javed et al.2022). *Parthenium hysterophorus* contains other phytochemicals such as alkaloids, steroids, glycosides, saponins (Marimuthu & Ravi, 2014). The biological effects of the species are due to its allelochemicals, which include phenolics and terpenoids, with sesquiterpene lactone parthenin being a major component. Parthenin is responsible for cytotoxic and antitumor activities. *Parthenium* mainly contains nutrients, phenolics, organic acids, and sesquiterpene lactones (Pandey et al. 2009).

##### **Anti-oxidant assay :**

The DPPH radical scavenging experiment was used to evaluate the extracts' antioxidant capacity. A 0.1 mM DPPH solution in 95% ethanol was prepared for this purpose. Next, 3 mL of the sample (ZnO NPs) in ethanol at a concentration of 100 µg/mL was mixed with 1 mL of this solution. After giving the mixture a good shake, it was allowed to sit at room temperature for half an hour. An UV-Vis spectrophotometer was then used to detect the absorbance at 517 nm. The experiment was conducted three times using ascorbic acid as the reference standard. Stronger free radical scavenging activity was indicated by the mixture's lower absorbance. This formula was used to determine the percentage of DPPH scavenging or inhibition :

DPPH scavenging effect (%) or Percent inhibition =  $A_0 - A_1 / A_0 \times 100$

Where, A0 = Absorbance of control reaction and A1 = Absorbance of test sample (Rai et al., 2021).

##### **Anti-cancer assay :**

The MDAMB231 and K562 cell lines were cultured at a concentration of ( $1 \times 10^4$ ) cells/ml in culture media for 24 hours at 37°C with 5% CO<sub>2</sub>. In a 96-well plate, cells were seeded at ( $1 \times 10^4$ ) cells/well in 100 µl of culture media containing various sample concentrations (20, 40, 60, 80, 100 µg/mL). The cell line and DMSO (0.2% in PBS) were used as controls. All experiments were carried out in triplicate. Control samples were utilized to assess cell survival. After 24 hours of incubation at 37°C with 5% CO<sub>2</sub>, remove the media and add 20 µl of MTT reagent (5 mg/ml in PBS). The cells were cultured for an additional four hours. Formazan crystals generated by live cells were viewed under a microscope, as alive cells transformed yellow MTT to dark formazan. After removing the medium, add 200 µl of DMSO and incubate at 37°C for 10 minutes (cover with foil). Each sample's absorbance was measured at 550 nm using a microplate reader (Mosmann, 1983; Hansen et al., 1989).

#### **RESULT AND DISCUSSION :**

##### **Synthesis of ZnO NPs :**

ZnO is an inorganic compound which occurs rarely in nature. It is generally found in crystalline form. The synthesis of ZnONPs was indicated by a color change in the plant extract. Over time, the reaction mixture changed from whitish yellow to brown (Naseer et al., 2020).

##### **U.V. Visible Spectroscopy :**

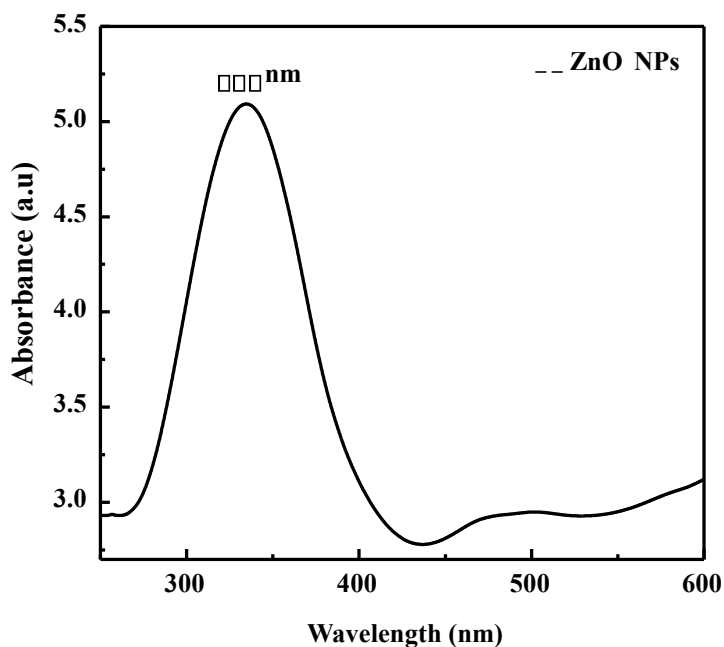


Figure 1. Shows the absorption spectrum of ZnO NPs of *Parthenium hysterophorus*.

The UV absorption spectrum of the synthesized zinc oxide nanoparticles (ZnO-NPs) ranged from 250 to 600 nm, with the highest absorption observed at 330 nm (Galedari&Teimouri,

2020). Eg (eV) = 1240/Wavelength in nm This formula was use to calculate band gap energy which is 3.75 eV.

Fourier Transform Infrared Spectroscopy (FTIR) :

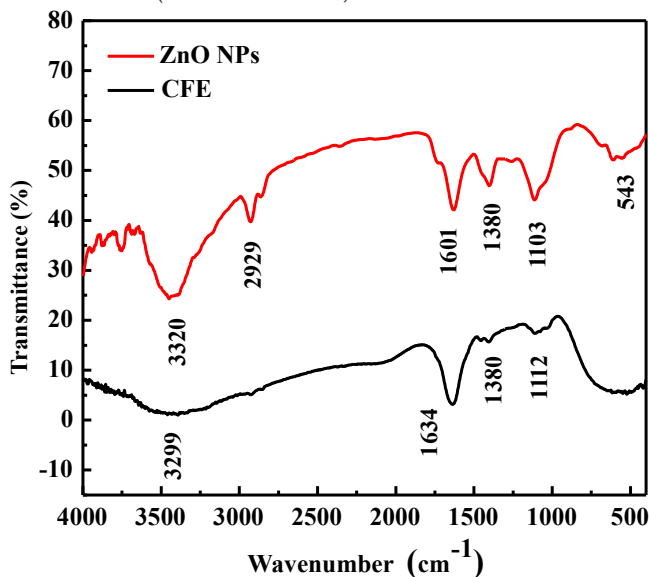


Figure 2. Shows The IR spectra of *Parthenium hysterophorus* aqueous extract and ZnO nanoparticles were compared using infrared spectrometry.

Key functional groups were identified by FTIR analysis of the floral extract of *Parthenium hysterophorus*. These included C=C stretching (aromatic compounds) at 1634  $\text{cm}^{-1}$ , C-H bending (alkanes or alkyl groups) at 1380  $\text{cm}^{-1}$ , C-O stretching (ethers or esters) at 1112  $\text{cm}^{-1}$ , and O-H stretching (alcohols or phenols) at 3299  $\text{cm}^{-1}$ . O-H stretching at 3320  $\text{cm}^{-1}$ , C-H stretching at 2929

$\text{cm}^{-1}$ , C=C stretching at 1601  $\text{cm}^{-1}$ , C-H bending at 1380  $\text{cm}^{-1}$ , and C-O stretching at 1103  $\text{cm}^{-1}$  were all comparable functional groups that were slightly shifted for ZnO nanoparticles made from the flower extract. Zn-O stretching was also confirmed by the identification of a new signal at 543  $\text{cm}^{-1}$ , which indicates the creation of ZnO nanoparticles. Peak shifts show interactions between ZnO and the extract's biomolecules during the production of nanoparticles (Nzilu et al., 2024).

X-ray diffraction (XRD):

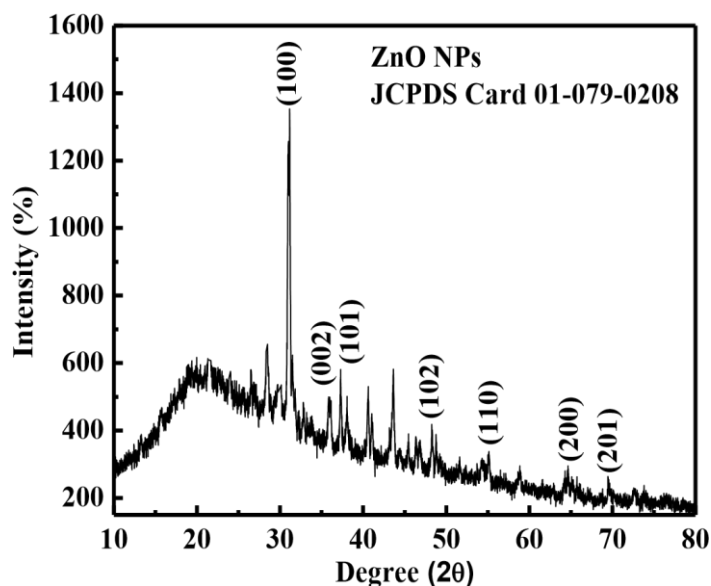


Figure 3. Shows The crystalline structure of synthesized ZnO NPs, illustrated using measured XRD diffraction patterns. The XRD pattern of ZnO nanoparticles (ZnO-NPs) matched the Miller indices and reference data for ZnO-NPs, indicating a polycrystalline structure with a hexagonal wurtzite shape. The nanoparticles, synthesized using the aqueous leaf extract of *Parthenium hysterophorus*, were consistent with the JCPDS reference card (01-079-0208). The XRD peaks appeared at 30.56, 34.44, and 36.42, corresponding to the Miller indices (100), (002), and (101), respectively. The crystallite size was calculated using the Debye-Scherrer formula:

$$D = \lambda / \beta \cos \theta$$

Here,  $k=0.9$  (constant),  $\lambda = 1.54 \text{ \AA}$  (Cu K $\alpha$  radiation wavelength),  $\beta$  is the peak's FWHM (in radians),  $\theta$  is the diffraction angle, and  $D$  is the crystal size. The crystallite size of ZnO-NPs was calculated to be 16.60 nm (AlWadi et.al., 2021).

Scanning Electron Microscopy (SEM) :

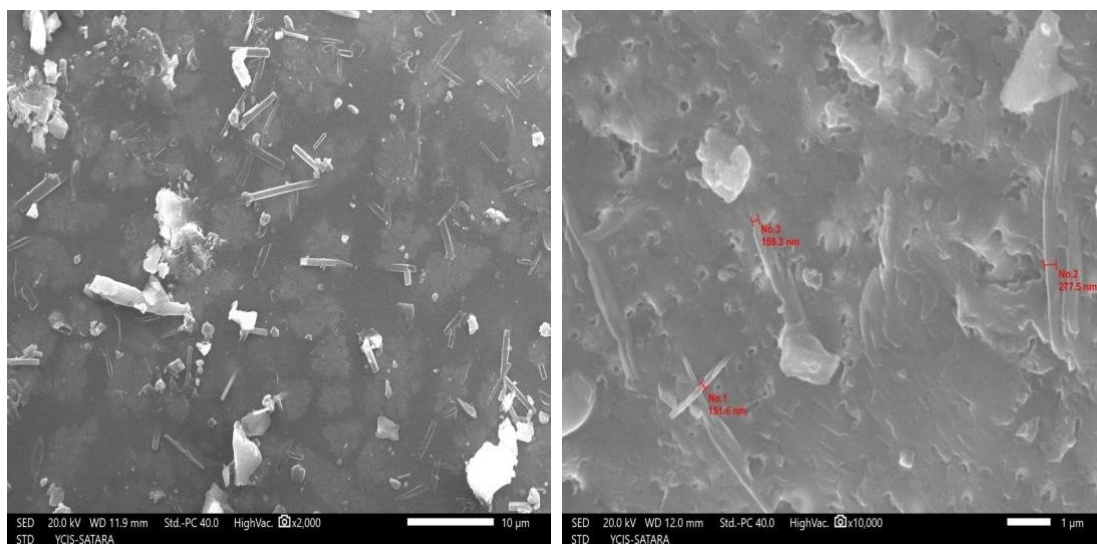


Figure 4. Shows the morphology of prepared ZnO NPs of *Parthenium hysterophorus* Floral extract.

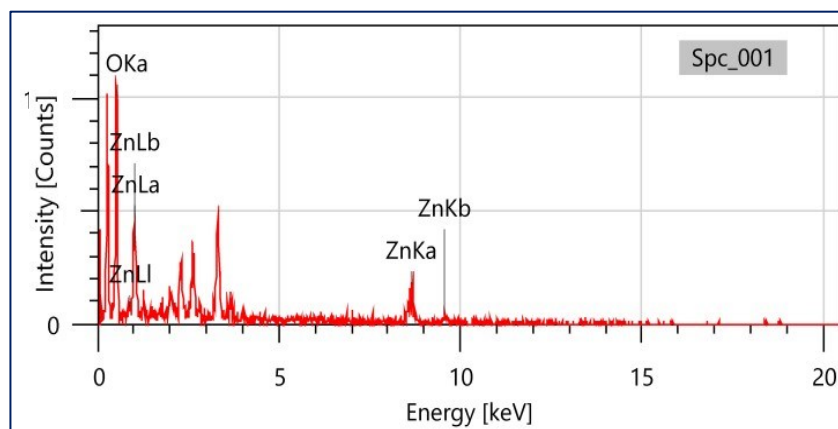


Figure 5. Shows EDS Spectrum of ZnO NPs of *Parthenium hysterophorus*

| Element | Line | Mass%                | Atom%      |
|---------|------|----------------------|------------|
| O       | K    | 53.83±2.17           | 82.65±3.33 |
| Zn      | K    | 46.17±4.41           | 17.35±1.66 |
| Total   |      | 100.00               | 100.00     |
| Spc_001 |      | Fitting ratio 0.6912 |            |

Figure 6. Shows elemental weight of ZnO NPs of *Parthenium hysterophorus*

As seen in Figure 4. ZnONPs exhibit in spherical, rod and irregular in shape. Sample was coated with a 4 nm gold layer to avoid charging effects during analysis. The nanoparticles have a relatively smooth surface, with some rough patches or facets visible. They show slight agglomeration, a common occurrence in dry powder form. Their sizes range from 50 nm to 200 nm, and

they display diverse shapes, including spherical, rod-like, and irregular structures. The size distribution is non-uniform, with noticeable variation in particle sizes (Liu et al., 2023). Figure 5. And 6. Contains EDS (Energy dispersive spectroscopy) giving confirmation of the desirable groups are present in Nanoparticles that are zinc (Zn) & oxygen (O).

**Phytochemical Analysis :**

Table 1. Shows Phytochemical analysis of ZnO NPs of *Parthenium hysterophorus*

| Sr.No. | Tests   | Observation         | Inference                 |
|--------|---|---------------------|---------------------------|
| 1.     | Extract Powder + Picric acid                          | Yellow color        | Presence of alkaloid      |
| 2.     | Extract Powder + Conc. H <sub>2</sub> SO <sub>4</sub> | Reddish brown color | Presence of steroids      |
| 3.     | Extract Powder + Aq. FeCl <sub>3</sub>                | Pale brown colour   | Absence of flavonoids     |
| 4.     | Extract Powder + Iodine solution                      | Brown colour        | Absence of starch         |
| 5.     | Extract Powder + Ammonia solution                     | No blood red colour | Absence of anthroquinone  |
| 6.     | Extract Powder + Aq. 5% KOH                           | Yellow color        | Presence of anthroquinone |
| 7.     | Extract Powder + NaOH                                 | Yellow color        | Presence of flavonoid     |
| 8.     | Extract Powder + Aq. AgNO <sub>3</sub>                | White precipitate   | Presence of protein       |

Bioactive compounds like alkaloids, flavonoids, tannins, saponins, terpenoids, and phenols are frequently identified through phytochemical analysis. When zinc oxide nanoparticles (ZnO-NPs) are combined with phytochemical compounds, the behavior of *Parthenium hysterophorus* ZnO nanoparticles with

various chemicals revealed positive results for alkaloids, steroids, anthroquinone, flavonoids, and protein.

**Antioxidant Activity :**

Table 2. Showing the Antioxidant Activity of ZnO NPs

|                        | % of inhibition |         |
|------------------------|-----------------|---------|
| Concentration (µg /ml) | Ascorbic acid   | ZnO NPs |
| 200                    | 98              | 81      |
| 400                    | 96              | 43      |
| 600                    | 94              | 39      |
| 800                    | 93              | 4       |
| 1000                   | 91              | 2       |

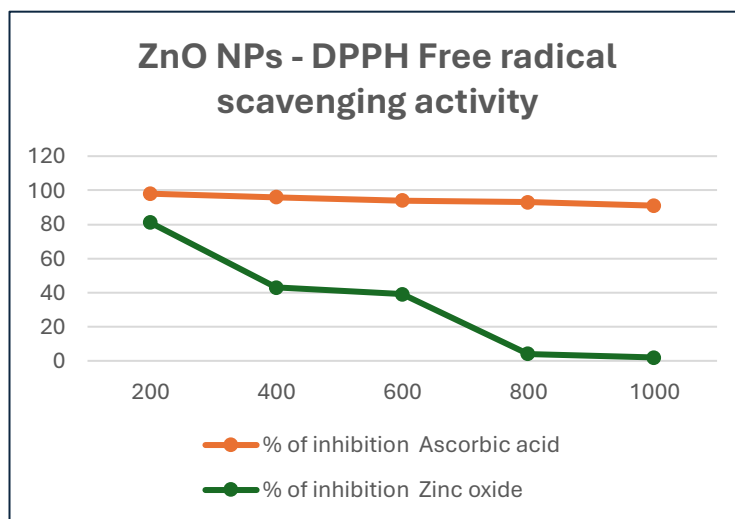


Figure 7. Shows Free radical scavenging activity of ZnO NPs of *Parthenium hysterophorus*

Table 2 confirmed that ZnO NPs exhibit good response in DPPH assay when compared with standard ascorbic acid. The DPPH scavenging assay, which is widely used to determine reducing agents and examine free radical scavenging behavior, was used to determine the antioxidant activity of ZnO NPs. ZnO NPs and standard ascorbic acid exhibit 98% and 81% free radical scavenging activity, respectively.

#### Anti-cancer Activity:

At various concentrations, ZnO nanoparticles (NPs) exhibited a percentage of inhibition, averaging 78.65%, against the K562 blood cancer cell line, compared to the standard drug 5-Fluorouracil (5FU). Based on the IC<sub>50</sub> value and the percentage of inhibition, it was observed that ZnO NPs demonstrated significant anticancer activity against blood cancer. Table 3 and Figure 8 details the IC<sub>50</sub> values and percentage of inhibition for K562 cells in comparison to 5FU. The data presented in Table 4

and Figure series 9 illustrate the relationship between IC<sub>50</sub> and inhibition concentration. At various concentrations, ZnO nanoparticles (NPs) exhibited a high percentage of inhibition, averaging 91.25 %, against the MDAMB231 Breast cancer cell line, compared to the standard drug 5FU. Based on the IC<sub>50</sub> value and the percentage of inhibition, it was observed that ZnO NPs demonstrated significant anticancer activity against Breast cancer. Table 4 details the IC<sub>50</sub> values and percentage of inhibition for MDAMB231 cells in comparison to 5FU. Table 5 presents the quantification of cell viability in terms of percentage inhibition for the NRK52E cell line in response to ZnO NPs. Across various concentrations, ZnO NPs exhibited a low percentage of inhibition against the NRK52E normal cell line, comparable to the standard drug 5FU. Based on the observed percentage of inhibition and viability, ZnO NPs are unlikely to be harmful to normal cells.

#### Anticancer activity against K562 (Blood cancer) cell lines :

Table 3. Shows Anticancer activity of ZnO NPs against K562 (Blood cancer) cell lines

| Sr. No. | Sample Code               | Concentration (µg/ml)       | O.D. at 550 nm                            |   |   | Mean                                      | % Inhibition of                               | % Viability of                                 | IC <sub>50</sub> (µg/ml) |
|---------|---------------------------|-----------------------------|---|---|---|---|---|--|--------------------------|
| 1.      | Control                   | -                           | 1.819                                     |   |   | -   | -   | -  | -                        |
| 2.      | Standard (5-Fluorouracil) | 20<br>40<br>60<br>80<br>100 | 1.761<br>1.542<br>0.911<br>0.764<br>0.532 | 1.759<br>1.544<br>0.913<br>0.762<br>0.534 | 1.764<br>1.540<br>0.909<br>0.766<br>0.530 | 1.761<br>1.542<br>0.911<br>0.764<br>0.532 | 3.18%<br>15.22%<br>49.91%<br>57.99%<br>70.75% | 96.82%<br>84.78%<br>50.09%<br>42.01%<br>29.25% | 61.25                    |
| 3.      | ZnO NPs                   | 20<br>40<br>60<br>80<br>100 | 1.698<br>1.432<br>1.304<br>0.872<br>0.811 | 1.699<br>1.433<br>1.303<br>0.870<br>0.811 | 1.698<br>1.434<br>1.307<br>0.873<br>0.811 | 1.698<br>1.433<br>1.305<br>0.871<br>0.811 | 6.65%<br>21.22%<br>28.25%<br>52.11%<br>55.41% | 93.35%<br>78.78%<br>71.75%<br>47.89%<br>44.59% | 78.65                    |

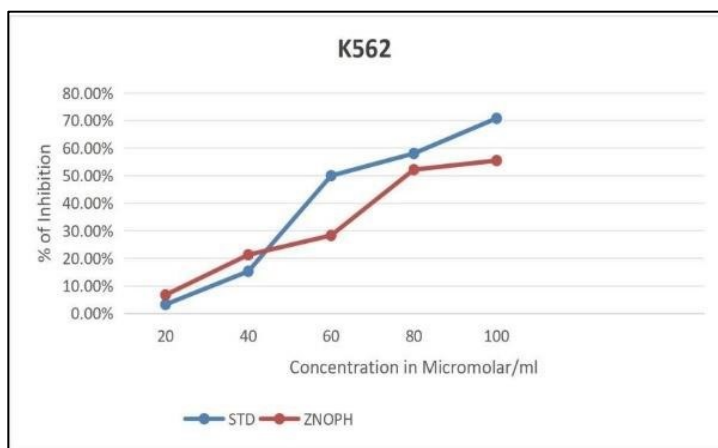


Figure 8. Shows Anticancer activity of ZnO NPs against K562 (Blood cancer) cell lines

Table 4. Shows Anticancer activity of ZnO NPs against MDMB231 (Breast cancer) cell lines

Anticancer activity against MDMB231 (Breast cancer) cell lines :

| Sr. No. | Sample Code               | Concentration (µg/ml)       | O.D. at 550 nm                            |   |   | Mean                                      | % Inhibition                                   | % Viability                                    | IC50 (µg/ml) |
|---------|---------------------------|-----------------------------|---|---|---|---|--|--|--------------|
| 1.      | Control                   | -                           | 1.549                                     |   |   | -   | -  | -  | -            |
| 2.      | Standard (5-Fluorouracil) | 20<br>40<br>60<br>80<br>100 | 1.320<br>1.098<br>0.841<br>0.624<br>0.491 | 1.320<br>1.098<br>0.840<br>0.624<br>0.492 | 1.321<br>1.099<br>0.840<br>0.624<br>0.491 | 1.320<br>1.098<br>0.840<br>0.624<br>0.491 | 14.78%<br>29.11%<br>45.77%<br>59.71%<br>68.30% | 85.22%<br>70.89%<br>54.23%<br>40.29%<br>31.70% | 62.25        |
| 3.      | ZnO NPs                   | 20<br>40<br>60<br>80<br>100 | 1.362<br>1.277<br>1.055<br>0.953<br>0.731 | 1.362<br>1.278<br>1.055<br>0.953<br>0.731 | 1.362<br>1.277<br>1.055<br>0.953<br>0.731 | 1.362<br>1.277<br>1.055<br>0.953<br>0.731 | 12.07%<br>17.55%<br>31.89%<br>38.47%<br>52.80% | 87.93%<br>82.45%<br>68.11%<br>61.53%<br>47.20% | 91.25        |

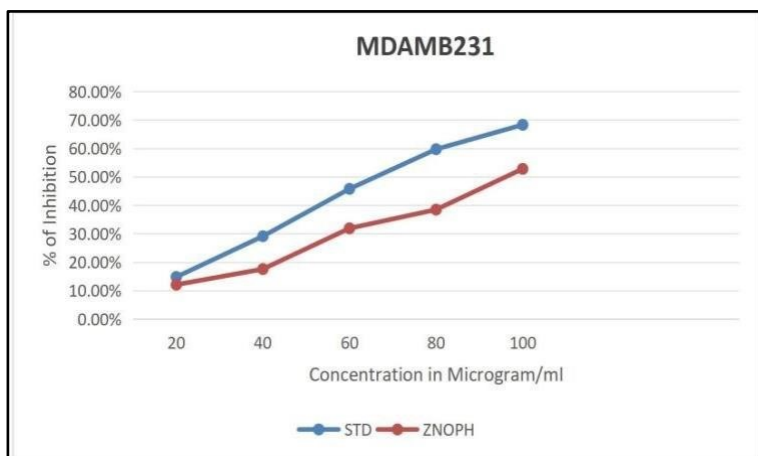


Figure 8. Shows Anticancer activity of ZnO NPs against MDAMB231 (Breast cancer) cell lines

Anticancer activity against NRK52E Normal kidney cell lines :

Table 5. Shows Anticancer activity of ZnO NPs against NRK52E Normal Kidney cell lines



| Sr. No. | Sample Code               | Concentration (µg/ml) | O.D. at 550 nm |       |       | Mean         | % of Inhibition | % of Viability | IC50 (µg/ml) |
|---------|---------------------------|-----------------------|----------------|-------|-------|--------------|-----------------|----------------|--------------|
| 1.      | Control                   | -                     | 1.532          |       |       | -            | -               | -              | -            |
| 2.      | Standard (5-Fluorouracil) | 20                    | 1.453          | 1.452 | 1.454 | <b>1.453</b> | <b>5.15%</b>    | <b>94.84%</b>  | <b>NE</b>    |
|         |                           | 40                    | 1.397          | 1.396 | 1.395 | <b>1.396</b> | <b>8.87%</b>    | <b>91.13%</b>  |              |
|         |                           | 60                    | 0.386          | 1.387 | 1.388 | <b>1.387</b> | <b>9.46%</b>    | <b>90.54%</b>  |              |
|         |                           | 80                    | 0.369          | 1.368 | 1.369 | <b>1.368</b> | <b>10.70%</b>   | <b>89.30%</b>  |              |
|         |                           | 100                   | 0.350          | 1.352 | 1.350 | <b>1.350</b> | <b>11.87%</b>   | <b>88.12%</b>  |              |
| 3.      | ZnO NPs                   | 20                    | 1.421          | 1.419 | 1.423 | <b>1.421</b> | <b>7.24%</b>    | <b>92.76%</b>  | <b>NE</b>    |
|         |                           | 40                    | 1.325          | 1.327 | 1.323 | <b>1.325</b> | <b>13.51%</b>   | <b>86.49%</b>  |              |
|         |                           | 60                    | 1.302          | 1.300 | 1.305 | <b>1.302</b> | <b>15.01%</b>   | <b>84.99%</b>  |              |
|         |                           | 80                    | 1.300          | 1.300 | 1.303 | <b>1.301</b> | <b>15.07%</b>   | <b>84.93%</b>  |              |
|         |                           | 100                   | 1.215          | 1.213 | 1.217 | <b>1.215</b> | <b>20.69%</b>   | <b>79.31%</b>  |              |

**\*NE =Not Evaluable**

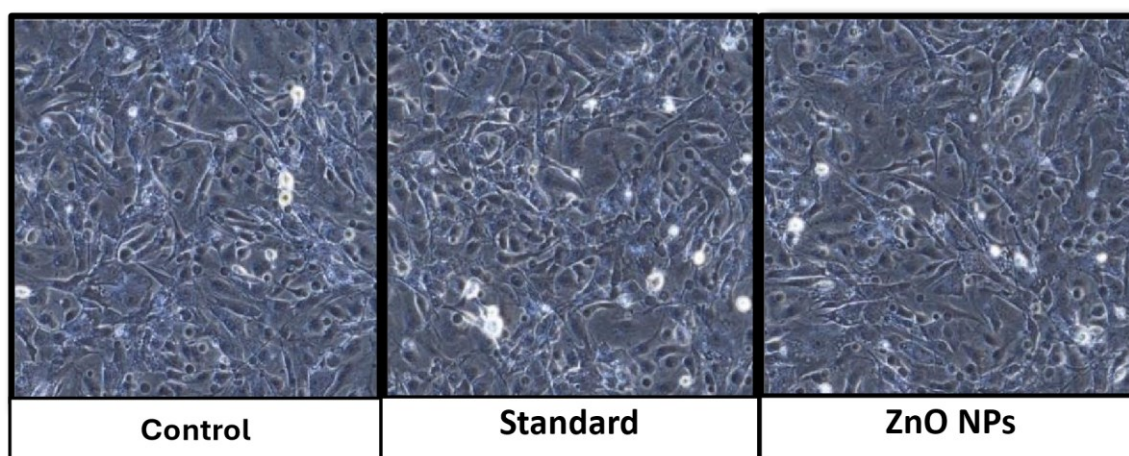


Figure 9. Shows Anticancer activity of ZnO NPs against NRK52E Normal Kidney cell lines



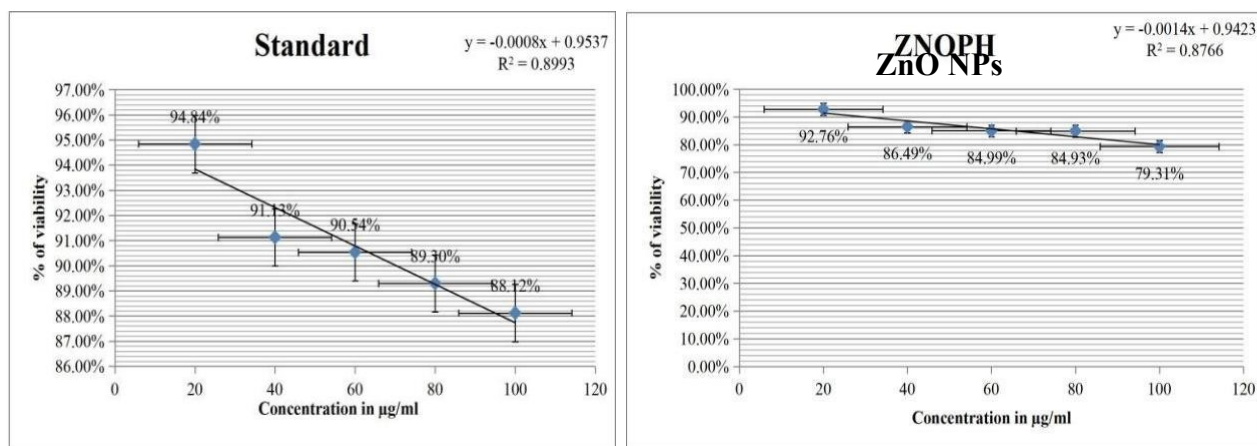


Figure 10. Shows Anticancer activity of ZnO NPs against NRK52E Normal Kidney cell lines

#### ACKNOWLEDGEMENT:

We would like to sincerely thank our guide and research advisors for their important advice, helpful criticism, and unwavering support during this project. Their knowledge and support have greatly influenced the direction of this study. We are also grateful to the Department of Microbiology at the Yashwantrao Chavan Institute of Science, Satara, for providing the tools and a supportive setting needed to carry out this investigation.

#### REFERENCES

- Saha, B., Koley, S., Khwairakpan, M., & Kalamdhad, A. S. (2022, December). Comparative study between mono-digestion and co-digestion of terrestrial weed (*Parthenium hysterophorus*). *Cleaner Engineering and Technology*, 11, 100560. <https://doi.org/10.1016/j.clet.2022.100560>
- Patel, S. (2011, April 27). Harmful and beneficial aspects of *Parthenium hysterophorus*: an update. *3 Biotech*, 1(1), 1-9. <https://doi.org/10.1007/s13205-011-0007-7>
- Bagchi A, Raha A, Mukherjee P. A complete review on *Parthenium hysterophorus* Linn. *International Journal of Recent Advance Pharmaceutical Research*. 2016;6(1):42-49.
- Kumar, S., Mishra, A., & Pandey, A. K. (2013, May 30) Antioxidant mediated protective effect of *Parthenium hysterophorus* against oxidative damage using in vitro models. *BMC Complementary and Alternative Medicine*, 13(1). <https://doi.org/10.1186/1472-6882-13-120>
- Oudhia, P. (2001). Medicinal uses of Congress weed *Parthenium hysterophorus* L.: A Review. *ECOLOGY ENVIRONMENT AND CONSERVATION*, 7, 175-177.
- Sharif, N. (2021, December 10), Antimicrobial activity of *Parthenium hysterophorus* against five bacterial strains. *Pure and Applied Biology*, 10(4). <https://doi.org/10.19045/bspab.2021-100146>
- Kumar, S., Pandey, S., & Pandey, A. K. (2014). In Vitro Antibacterial, Antioxidant, and Cytotoxic Activities of *Parthenium hysterophorus* and Characterization of Extracts by LC-MS Analysis. *BioMed Research International*, 2014, 1-10. <https://doi.org/10.1155/2014/495154>
- Jaiswal, J., Singh, N., Gupta, V. K., Doharey, P. K., Siddiqi, N. J., & Sharma, B. (2022, September) Pharmacological Chemistry and Biomedical Implications of Chemical Ingredients from *Parthenium hysterophorus*. *Current Topics in Medicinal Chemistry*, 22(23), 1950-1965 <https://doi.org/10.2174/1568026622666220307145027>
- Picman, A. K., Elliott, R. H., & Towers, G. H. N. (1981). Cardiac-inhibiting properties of the sesquiterpene lactone, parthenin, in the migratory grasshopper, *Melanoplus sanguinipes*. *Canadian Journal of Zoology*, 59(2), 285-292. <https://doi.org/10.1139/z81043>
- Daizy R. Batish, H.P. Singh, R.K. Kohli, D.B. Saxena, Shalinder Kaur Alleopathic effects of parthenin against two weedy species, *Avena fatua* and *Bidens pilosa*, *Environmental and Experimental Botany*, Volume 47, Issue 2, 2002, Pages 149-155, ISSN 0098-8472 [https://doi.org/10.1016/S0098-8472\(01\)00122-8](https://doi.org/10.1016/S0098-8472(01)00122-8)
- Batish, D., Singh, H., Saxena, D. and Kohli, R. 2002. Weed suppressing ability of parthenin a sesquiterpene lactone from *Parthenium hysterophorus*. *New Zealand Plant Protection*. 55, (Aug. 2002), 218-221. DOI: <https://doi.org/10.30843/nzpp.2002.55.3893>
- Parashar, V., Parashar, R., Sharma, B., & Pandey, A. C. (2009). *Parthenium* leaf extract mediated synthesis of silver nanoparticles: a novel approach towards weed utilization. *Digest Journal of Nanomaterials & Biostructures (DJNB)*, 4(1).
- P. Rajiv, Sivaraj Rajeshwari, Rajendran Venckatesh, Bio-Fabrication of zinc oxide nanoparticles using leaf extract of *Parthenium hysterophorus* L. and its size-dependent antifungal activity against plant fungal pathogens, *Spectrochimica Acta Part A: Molecular and Biomolecular Spectroscopy*, Volume 112, 2013, Pages 384-387, ISSN 1386-1425, <https://doi.org/10.1016/j.saa.2013.04.072>
- Meenakshi, D. U., Nandakumar, S., Ganesan, P., Salim, L., Sweet, J. P., & Khan, S. A. (2024). Zinc oxide nanoformulations for cancer therapy. In *Apple Academic Press eBooks* (pp. 39-79). <https://doi.org/10.1201/9781003538455-2>
- Saini, K., Gupta, K., Shekhawat, K. S., & Mathur, J. (2024). Exploration of the catalytic, anti-bacterial, and anti-oxidant capabilities of environmentally conscious zinc oxide nanoparticles synthesized using *Citrus sinensis*. *Journal of the Indian Chemical Society*, 101(9), 101232. <https://doi.org/10.1016/j.jics.2024.101232>
- Iqbal, J., Khan, A. A., Aziz, T., Ali, W., Ahmad, S., Rahman, S. U., Iqbal, Z., Dablood, A. S., Alruways, M. W., Almalki, A. A., Alamri, A. S., & Alhomrani, M. (2022). Phytochemical Investigation, Antioxidant Properties and In Vivo Evaluation of the Toxic Effects of *Parthenium hysterophorus*. *Molecules*, 27(13), 4189. <https://doi.org/10.3390/molecules27134189>
- Alfaro Jiménez, M. A., Zugasti Cruz, A., Silva Belmares, S. Y., Ascacio Valdés, J. A., & Sierra Rivera, C. A. (2022). Phytochemical and Biological Characterization of the Fractions of the Aqueous and Ethanolic Extracts of *Parthenium hysterophorus*. *Separations*, 9(11), 359. <https://doi.org/10.3390/separations9110359>

- Kumari, C., & Deepalakshmi, J. (2017). Qualitative and GC-MS Analysis of Phytoconstituents of *Parthenium hysterophorus* Linn. *Research Journal of Pharmacognosy and Phytochemistry*, 9(2), 105. <https://doi.org/10.5958/0975-4385.2017.00019.x>
- Tanwar, S. N., Parauha, Y. R., There, Y., Swart, H. C., & Dhoble, S. J. (2024). Plant-Based Biosynthesis of Metal and Metal Oxide Nanoparticles: An Update on Antimicrobial and Anticancer Activity. *ChemBioEng Reviews*. <https://doi.org/10.1002/cben.202400012>
- Anjum, S., Hashim, M., Malik, S. A., Khan, M., Lorenzo, J. M., Abbasi, B. H., & Hano, C. (2021). Recent Advances in Zinc Oxide Nanoparticles (ZnO NPs) for Cancer Diagnosis, Target Drug Delivery, and Treatment. *Cancers*, 13(18), 4570. <https://doi.org/10.3390/cancers1318457029>
- Alsagaby, S. A., Vijayakumar, R., Premanathan, M., Mickymaray, S., Alturaiki, W., AlBaradie, R. S., AlGhamdi, S., Aziz, M. A., Alhumaydhi, F. A., Alzahrani, F. A., Alwashmi, A. S., Abdulmonem, W. A., Alharbi, N. K., & Pepper, C. (2020). <p>Transcriptomics-Based Characterization of the Toxicity of ZnO Nanoparticles Against Chronic Myeloid Leukemia Cells</p> *International Journal of Nanomedicine*, Volume 15, 7901-7921. <https://doi.org/10.2147/ijn.s261636>
- Iqbal, J., Khan, A. A., Aziz, T., Ali, W., Ahmad, S., Rahman, S. U., Iqbal, Z., Dabool, A. S., Alruways, M. W., Almalki, A. A., Alamri, A. S., & Alhomrani, M. (2022). Phytochemical Investigation, Antioxidant Properties and In Vivo Evaluation of the Toxic Effects of *Parthenium hysterophorus*. *Molecules (Basel, Switzerland)*, 27(13), 4189. <https://doi.org/10.3390/molecules27134189>
- Krishnaveni Marimuthu, K. M., & Dhanalakshmi Ravi, D. R. (2014). Phytochemical analysis of *Parthenium hysterophorus* L. leaf.
- Pandey, D.K. (2009). Allelochemicals in *Parthenium* in response to biological activity and the environment.
- Rai, A. (2021). Antimicrobial, antioxidant and cytotoxic activity of green synthesized copper nanoparticle of *Parthenium hysterophorus* L. *INTERNATIONAL JOURNAL OF MULTIDISCIPLINARY RESEARCH AND ANALYSIS*, 04(02). <https://doi.org/10.47191/ijmra/v4-i2-01>
- Mosmann, T. (1983). Rapid colorimetric assay for cellular growth and survival: Application to proliferation and cytotoxicity assays. *Journal of Immunological Methods*, 65(1-2), 55-63. [https://doi.org/10.1016/0022-1759\(83\)90303-4](https://doi.org/10.1016/0022-1759(83)90303-4)
- Hansen, M. B., Nielsen, S. E., & Berg, K. (1989). Re-examination and further development of a precise and rapid dye method for measuring cell growth/cell kill. *Journal of immunological methods*, 119(2), 203-210. [https://doi.org/10.1016/0022-1759\(89\)90397-9](https://doi.org/10.1016/0022-1759(89)90397-9)
- Naseer, M., Aslam, U., Khalid, B., & Chen, B. (2020). Green route to synthesize Zinc Oxide Nanoparticles using leaf extracts of *Cassia fistula* and *Melia azadirach* and their antibacterial potential. *Scientific Reports*, 10(1). <https://doi.org/10.1038/s41598-020-65949-3>
- Galedari, S., & Teimouri, M. (2020). Study of the physicochemical properties and antibiofilm effects of synthesized zinc oxide nanoparticles using *Artemisia* plant. *International Journal of Basic Science in Medicine*, 5(3), 101-107. <https://doi.org/10.34172/ijbsm.2020.18>
- Nzilu, D., Madivoli, E., Makhani, D., Wanakai, S., Kirui, G., Mwangi, V., & Kareru, P. (2024). Synthesis and characterization of *Parthenium hysterophorus*-Mediated ZNO nanoparticles for methylene blue dye degradation. *Journal of Chemistry*, 2024, 1-19. <https://doi.org/10.1155/2024/1088430>
- AlWadi, A. (2021). Green Synthesis by *ZygophyllumCoccineum* Leaves Extract for Preparing ZnO Nanoparticles, and Characteristics Study. *Egyptian Journal of Chemistry*, 0(0), 0. <https://doi.org/10.21608/ejchem.2021.102312.4746>
- Liu, H., Li, Z., Yang, Y., Miao, G., & Han, Y. (2023). Effects of oxidation on physical and chemical structure of a low rank sub-bituminous coal during the spontaneous combustion latency. *Energy*, 272, 127122. <https://doi.org/10.1016/j.energy.2023.127122>